Ag–Ag_2O composite structure with tunable localized surface plasmon resonance as ultrastable, sensitive and cost-effective SERS substrate

Wenfeng Sun, Wenzuo Wei, Qingyou Liu, Tingzhen Yan, Qi Wang, Hui Lin, Chunxian Tao, Dawei Zhang, Ruijin Hong

PII: S0925-8388(20)32093-4

DOI: https://doi.org/10.1016/j.jallcom.2020.155729

Reference: JALCOM 155729

To appear in: *Journal of Alloys and Compounds*

Received Date: 9 April 2020

Revised Date: 18 May 2020

Accepted Date: 19 May 2020

Please cite this article as: W. Sun, W. Wei, Q. Liu, T. Yan, Q. Wang, H. Lin, C. Tao, D. Zhang, R. Hong, Ag–Ag_2O composite structure with tunable localized surface plasmon resonance as ultrastable, sensitive and cost-effective SERS substrate, *Journal of Alloys and Compounds* (2020), doi: https://doi.org/10.1016/j.jallcom.2020.155729.

Credit Author Statement

Wenfeng Sun: Writing - original draft, Software.

Wenzuo Wei: Review - editing, Investigation.

Qingyou Liu: Data curation.

Tingzhen Yan: Data curation.

Qi Wang: Data curation.

Chunxian Tao: Data curation.

Hui Lin: Formal analysis.

Dawei Zhang: Project administration, Validation.

Ruijin Hong: Writing - review & editing, Supervision.

Ag-Ag$_2$O composite structure with tunable localized surface plasmon resonance as ultrastable, sensitive and cost-effective SERS substrate

Wenfeng Sun[1], Wenzuo Wei[2], Qingyou Liu[3], Tingzhen Yan[1], Qi Wang[1], Hui Lin[1], Chunxian Tao[1], Dawei Zhang[1], Ruijin Hong[1]*

[1] Engineering Research Center of Optical Instrument and System, Ministry of Education and Shanghai Key Lab of Modern Optical System, University of Shanghai for Science and Technology, No.516 Jungong Road, Shanghai 200093, China.

[2] Institute of Physics, Univeristy of Rostock, Rostock 18059, Germany.

[3] Key Laboratory of High-temperature and High-pressure Study of the Earth's Interior, Institute of Geochemistry, Chinese Academy of Sciences, Guiyang 550081, China.

* Corresponding author.

E-mail address: rjhong@usst.edu.cn (R. Hong)

Abstract

Ag-Ag$_2$O composite structure, with fine tunability of localized surface plasmon resonance (LSPR), was fabricated by using Nd:YAG fiber pulsed laser ablation at ambient conditions. In this structure, tunable LSPR of Ag nanoparticles (NPs) with the wavelength from 384 nm to 486 nm was realized by varying the laser power to regulate both the oxidation degree and the spacing of Ag NPs. Moreover, Surface enhanced Raman scattering (SERS) was also observed due to the composite structure, which was demonstrated excellent stability and SERS sensitivity with the detectable concentration of Rhodamine B as low as 10^{-11} mol/L. The SERS substrates fabricated by laser ablation also exhibited favorable reproducibility and uniformity. The simulation results of finite difference time domain (FDTD) regarding the electric field distribution of all samples are in good agreement with those of above results.

Keywords: Ag nanoparticle films; oxidation; LSPR; SERS; FDTD

1. Introduction

Localized surface plasmon resonance (LSPR) is normally referred to the collective electron oscillation phenomenon between metal nanoparticles (NPs) at the time when the frequency of the incident light is equal to the vibration frequency of the conduction electrons [1, 2]. During LSPR, the interaction between light and surface plasmon polariton results in the high extinction coefficient and significant amplification of the electric field near the metal nanoparticle surface [3].With fine tunability of LSPR, metal nanostructure has a significant application in surface enhanced Raman scattering (SERS), especially, being SERS substrates [4].

Noble metals such as gold and silver (Ag) are desirable plasmonic materials to fabricate SERS substrates because of their stable chemical properties [5]. However, due to some disadvantages, i.e. high-cost of the former and easy-oxidizability of the latter [6], such materials have not been widely applied as SERS substrates. On the other hand, complicated and costly fabrication of them are still the matters that restrict the development in practical applications, even though the problem of silver can be solved by composite structure of Ag and semiconductors, i.e. Ag/TiO_2, Ag/ZnO, and Ag/SnO_2 [7-9].

Previous studies show that the frequency of LSPR is dependent on not only the shape, size, spacing and metal materials but also the dielectric constant of surrounding medium [10-12]. Interestingly, the partial oxidation in the surface of Ag NPs influences its local dielectric environment as well. Given the assumption that surface oxidation degree of Ag NPs could be regulated simply, the undesirable oxidizable characteristic of Ag NPs would possibly provide an effective way in regulating its plasmonic performance. Meanwhile, the oxide layer, i.e. Ag_2O, could also protect Ag NPs from the sulfuration and oxidation, further improving the stability of being SERS substrates. Our recent report shows that laser irradiation technique offers an effective way to tune LSPR property of Ag film, with the addition of Al buffer layer [13]. Still, the intensity of both LSPR peak intensity and corresponding SERS signal of those irradiated Ag-Al NPs are not strong enough. Alternative possibility is the pulsed laser ablation technique, an environment-friendly method that can fabricate metals NPs by focusing high energy pulsed laser on the metal target and generating a plasma pluma of ablated material [14, 15]. When this plasma condenses, NP thin films are formed on the blank cover glass [16, 17].

In this study, Ag-Ag_2O composite structure was designed and fabricated as an ultrastable and sensitive SERS substrate by pulsed laser-induced ablation technique. The LSPR frequency of Ag-Ag_2O composite structure can be effectively tuned by varying the laser power. The effect of laser ablation on the composition, morphology, resonance absorption and SERS performance of samples were also discussed. Furthermore, the electric field distribution of samples were calculated by finite difference time domain (FDTD).

2. Experiment

Ag thin film was grown on the BK7 substrate by electron beam evaporation. The thickness was about 100 nm monitored by an in situ quartz crystal microbalance. Following the deposition, the cover glass was overlaid on Ag thin film and ablated by an Nd:YAG fiber pulsed laser at ambient condition. Parameters of the pulsed laser were set as follow: laser scan speed of 600 mm/s, scanning line spacing of 0.01 mm, pulse width of 200 ns, frequency of 45 kHz and laser beam diameter of 0.01 mm, respectively. The power of fiber pulsed laser were set as 2, 4, 6, 8 and 10 W, which are corresponded to the denotation of S1-S5 for as-ablated samples, respectively. For comparison, we also investigated the Ag thin film in the research. The schematic diagram of the laser ablation is shown in Fig. 1.

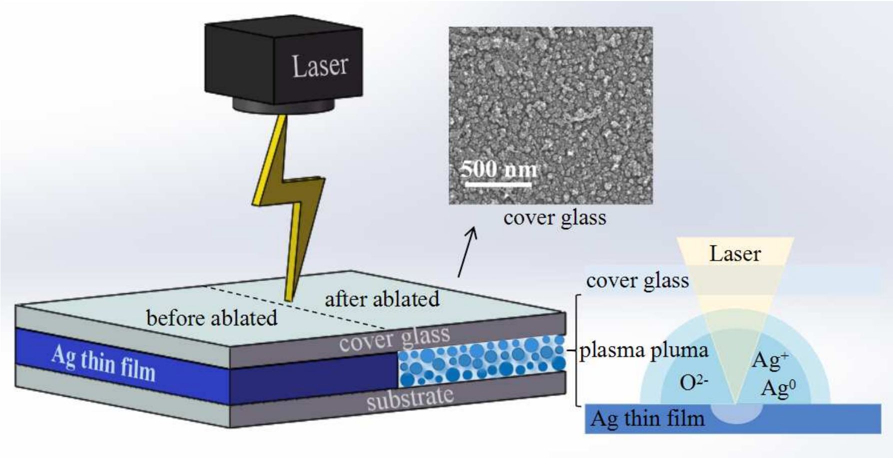

Fig. 1 A schematic diagram of the experiment process.

The phases of the samples were characterized by X-ray diffraction (XRD, Rigaku MiniFlex600 system, Japan). Surface analysis of the samples was conducted by the X-ray photoelectron spectroscopy (XPS, Thermo Scientific K-Alpha+). The surface morphology was analyzed through atomic force microscopy (AFM, XE-100, Park System) and scanning electron microscope (SEM) (S-4800, Hitachi). The absorption spectra were characterized by an UV-VIS-NIR spectrophotometer (Lambda 1050, Perkins Elmer). Raman signals were obtained by Raman spectroscopy (inVia Raman Microscope, Renishaw) with 633 nm laser excitation.

3. **Results and discussion**

3.1. Structural properties

The effect of laser ablation on the structure of samples is revealed in Fig. 2. A strong diffraction peak can be observed at 38.0° (2θ) in all the samples, corresponding to the (111) crystallographic plane of silver (JCPDS: 04-0783). Generally, for non-epitaxial deposition on a substrate, the film surface tends to be either a (001) or (111) plane owing to the minimum surface free energy in these planes [18]. Compared with the sharp diffraction profile of as-deposited Ag thin film, the diffraction intensities of as-ablated samples are significantly reduced due to the thinner thickness after laser ablation. No obvious peak-shift was observed in samples before and after laser ablation. For the as-ablated samples, besides the major diffraction peak at about 38.0° (2θ), there is another diffraction peak at 32.8° (2θ) corresponding to Ag_2O (111) plane (JCPDS: 41-1104). With the laser power increasing,the diffraction intensity of Ag (111) slightly decreases, while those of Ag_2O (111) show an increased trend. This means the surface of as-ablated samples is prone to be oxidized at ambient conditions during the case of pulsed laser ablation. Meanwhile, the increase of Ag_2O diffraction intensity indicates that the oxidation of Ag NPs becomes gradually serious with the laser power increasing.

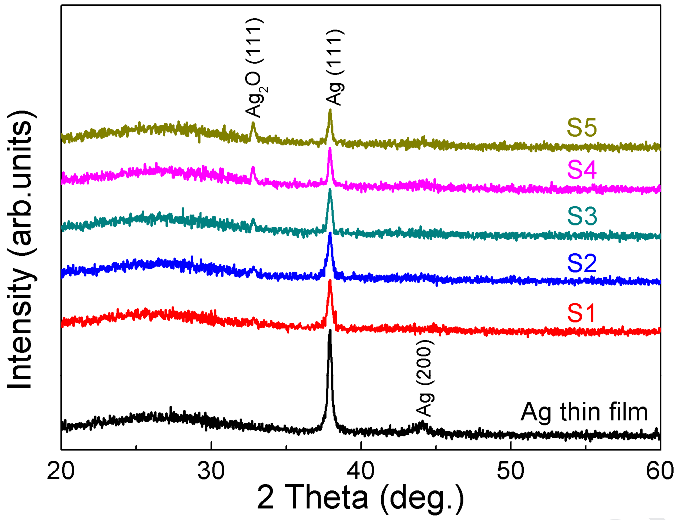

Fig. 2 XRD pattern of Ag thin film and as-ablated samples.

3.2.Composition and valence state

Fig. 3 shows the XPS spectra of as-ablated samples with various laser powers. The XPS spectra shape of as-ablated samples is similar to those reported by literature [19]. Two peaks can be observed in as-ablated samples, corresponding to Ag 3d$_{5/2}$ and Ag 3d$_{3/2}$, respectively. According to the literature [20], the Ag 3d$_{5/2}$ peak of Ag and Ag$_2$O appear at 368.2 eV and 367.8 eV, respectively. No obvious oxidation was detected in the Ag 3d$_{5/2}$ peak of as-ablated sample at 368.3 eV as laser power less than 2 W. The Ag 3d$_{5/2}$ peak of as-ablated sample shows blue shift with the increase of laser power, which confirms the oxidation degree of samples and is in accordance with the result of XRD.

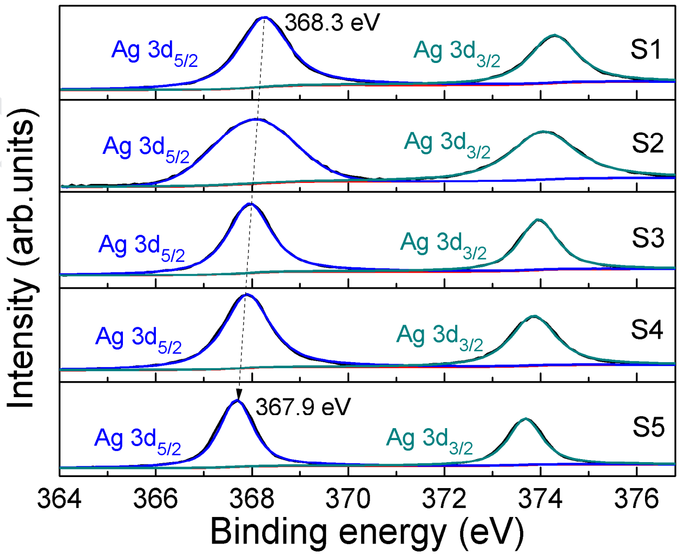

Fig. 3 XPS spectra of as-ablated samples.

3.3. Surface morphology

The AFM images of the Ag thin film and as-ablated samples are displayed in Fig. 4(a) and (b), respectively. It is obvious that the morphology of Ag thin film is smooth one. After the pulsed laser ablation, however, the smooth surface breakup into metallic NPs under the action of the thermo-elastic force from pulsed laser [21], attaching to the cover glass and thereby form orderly spheroidal structure on it [22]. According to Fig. 4(c), the root-mean-square surface roughness (Rq) values of as-ablated samples are 11.561, 12.164, 13.475, 13.991 and 14.895 nm, respectively. More laser energy was absorbed to form NPs with larger size along with the increase of laser power, thus gradually increasing the surface roughness of samples as well.

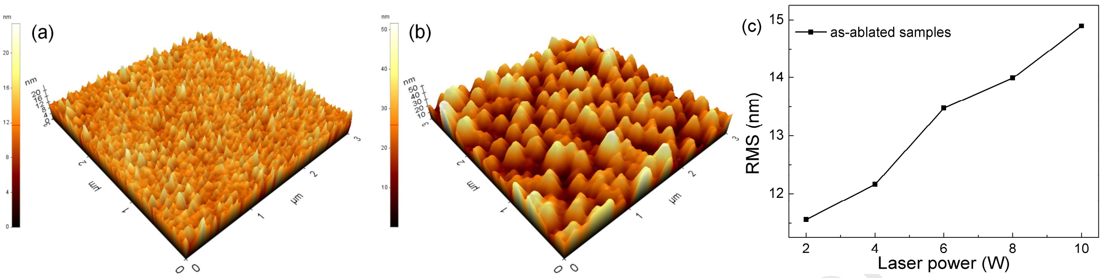

Fig. 4 The typical AFM images of (a) as-deposited Ag thin film and (b) the as-ablated Ag thin film. (c) The surface roughness of as-ablated samples.

Fig. 5 shows the corresponding SEM images of the as-ablated sample. The laser ablation process is found to have a profound effect on the morphology. The Ag NPs were densely distributed on the substrate with size of about 30-50 nm. Since this size range is much less than that of the incident wavelength (200-800 nm), the higher order oscillation modes are not considered in the analysis of absorption spectrum. With the laser power increasing, the spacing of NPs narrows gradually, and the state of aggregation increased. When the laser power increased up to 10 W, the deposited particles were so numerous that they were stacked on top of each other. However, with the laser power further increasing, the film surface was no longer uniform and a large number of particles were clustered together. It is worth noting that the excessive laser power led to a nonuniform stacking of NPs on the substrate, which negatively affected the SERS performance of samples [23].

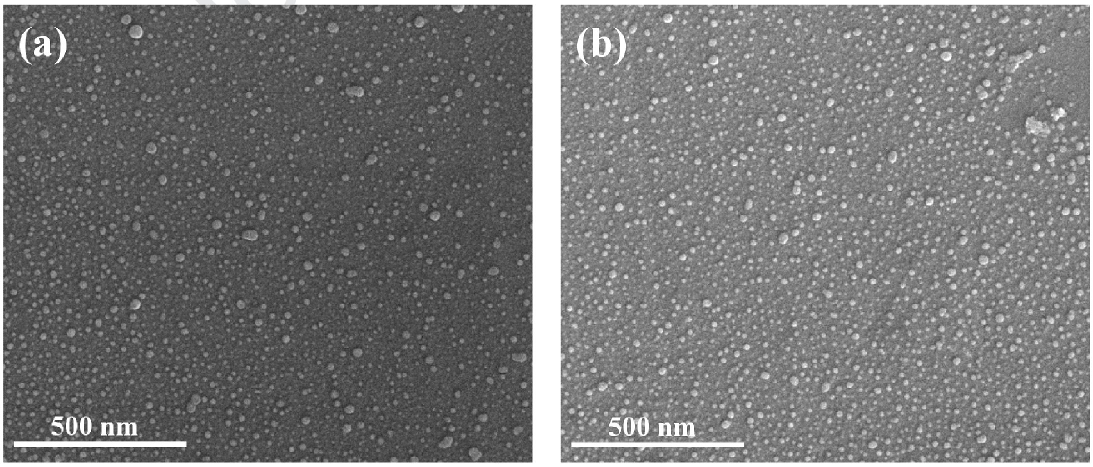

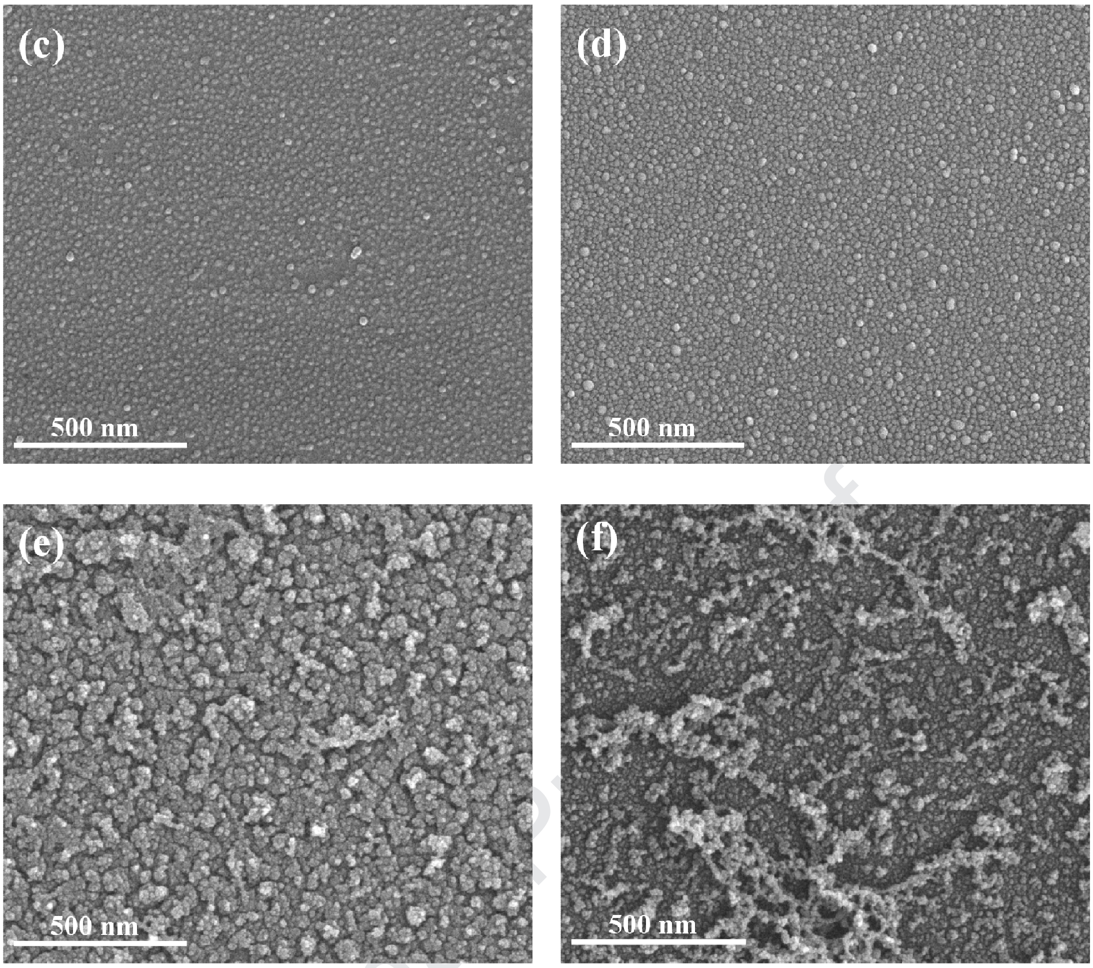

Fig. 5 SEM images of the as-ablated sample with laser of (a) 2 W, (b) 4 W, (c) 6 W, (d) 8 W, (e) 10 W, (f) 12 W.

3.4. Optical absorption

The optical absorption spectra of Ag thin film and as-ablated samples are shown in Fig. 6(a). Before laser ablation, Ag thin film shows strong resonance absorption intensity with broad absorption band due to consecutive topography of film [24]. After laser ablation, the localized electronic coherent oscillation was generated on the structured surface of as-ablated samples, leading to the resonance absorption peaks. The corresponding wavelength of absorption peak has an obvious red-shift from 384 nm to 486 nm with the increase of laser power, accompanying with the decreasing intensity of absorption peaks, as shown in Fig. 6(b).

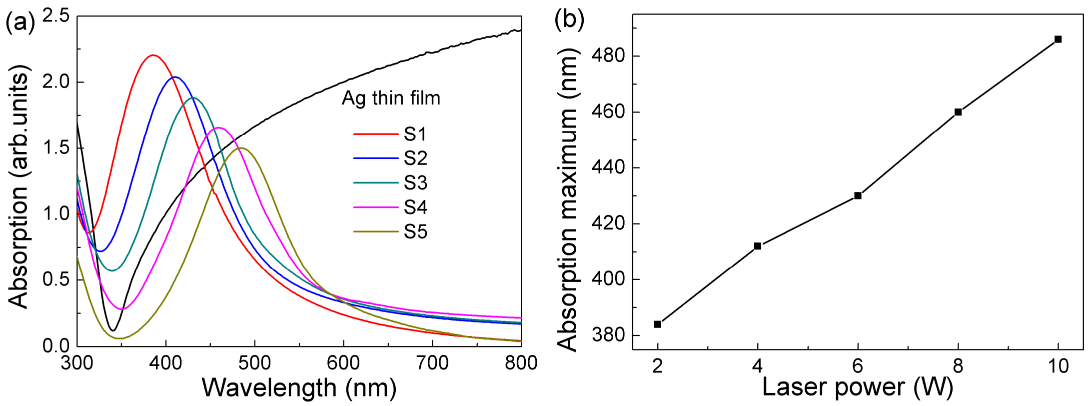

Fig. 6 (a) Optical absorption spectrum of Ag thin film and as-ablated samples, (b) Absorption maximum of every absorption curve.

The effective medium theory introduced by Maxwell-Garnett and Bruggeman can be used to research the absorption spectroscopy of spherical or ellipsoidal shapes nanostructure [25]. The as-ablated samples show a good performance in LSPR due to the regular nano-ellipsoid structure on the surface in comparison to Ag film with smooth surface. XRD and XPS results showed that the local dielectric environment of as-ablated samples varied accordingly with the increase of laser power. The LSPR wavelength is related to refractive index of the environmental medium based on the Drude mode [26]. The dielectric constant of surrounding medium increases as oxidation takes place in surface of Ag NPs, and the LSPR shifts to the longer wavelength accordingly [27]. Furthermore, when the unpolarized light beam was incident onto the sample perpendicularly, smaller spacing between NPs caused strong coupling effect. It also caused the red shift for absorption wavelength simultaneously [28]. The increase of Ag_2O content in as-ablated samples also leads to the decrease of absorption intensity. It is apparent that the LSPR performance can be tuned effectively by varying the laser powers.

3.5. SERS performance

In order to study the effect of laser power and oxidation on the potential application of plasmonic properties, all the samples were used as SERS substrates for probing Rhodamine B (Rh B) molecules. The Rh B molecule solutions with the concentration of 10^{-5} mol/L were spun onto the surface of samples. According to Fig. 7(a), there are three strong Raman peaks detected at about 1361, 1504 and 1648 cm^{-1}, assigned to C=C stretching modes of aromatic rings. The Raman signal scattering intensity from as-deposited Ag thin film was very weak, while the signal intensity of as-ablated sample was significantly enhanced with the increasing laser power. It is well known that the thermal stabilization of Ag is poor [29], so the stability of samples as SERS substrates should be evaluated. We restudied the SERS performance of Ag thin film and as-ablated samples after 90 days exposure. For convenience, the Ag thin film and as-ablated samples tested after 90 days were defined as Ag thin film’, S1’, S2’, S3’, S4’ and S5’. According to Fig. 7(c), the SERS spectra after 90 days exposure exhibit the same trend as those of the newly fabricated samples. Fig. 7(b) and (d) show the corresponding histogram of the intensity variation with error bar for

Fig. 7(a) and (c), respectively. The error bars are only 1-2% variation, which represent the standard deviation of Raman intensity in twelve measurements. With the increase of laser power, the Raman signal intensity of the as-ablated samples enhances obviously. The strong Raman peaks of Ag thin film and as-ablated samples at different days were compared in Fig. 7(e). It is obviously that the Raman signal of as-deposited Ag thin film disappeared after 90 days exposure, while no obvious changes in intensity for the as-ablated samples. Compared with as-deposited thin film, the thermal stability of as-ablated sample with Ag-Ag_2O structure was greatly improved.

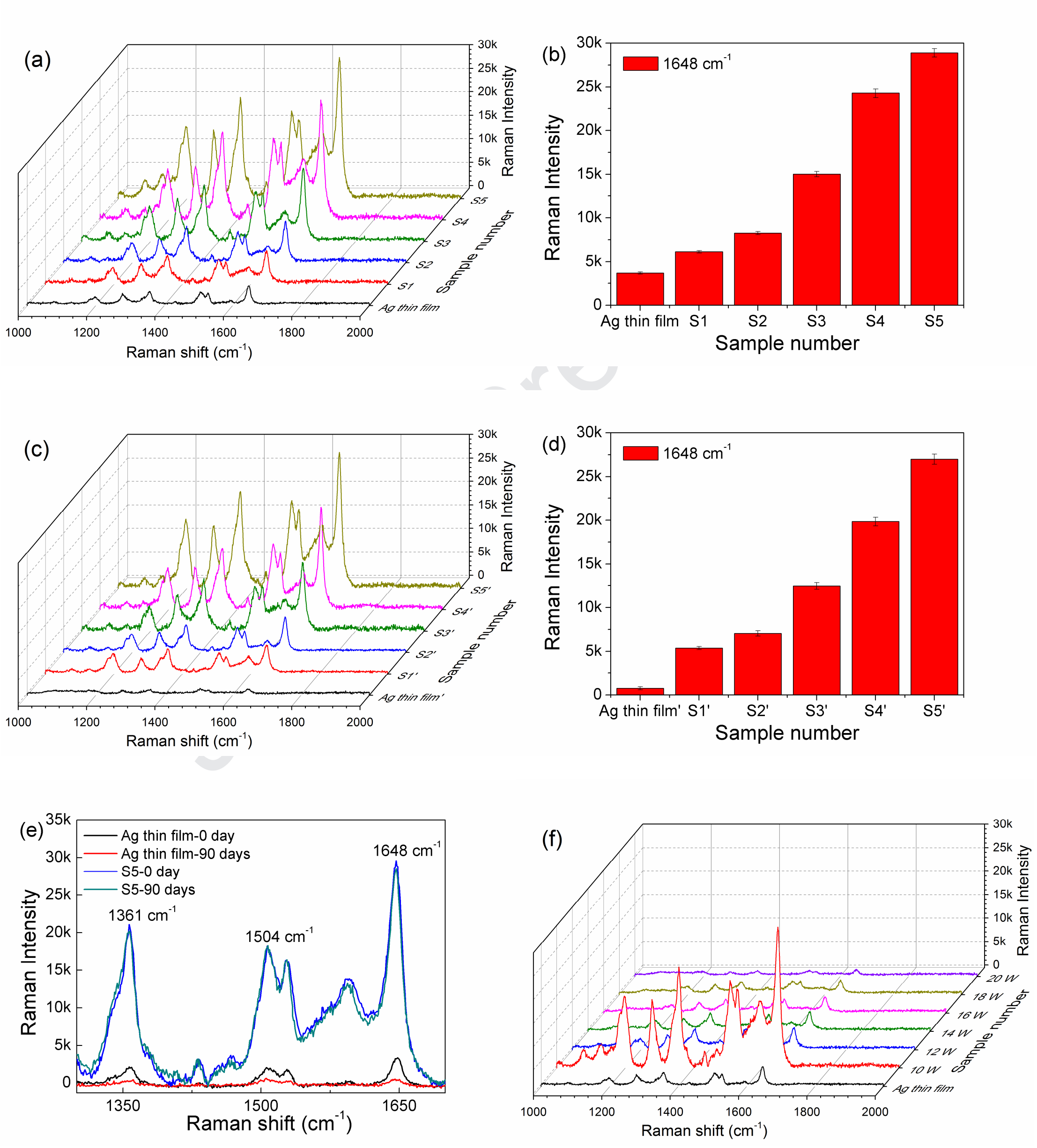

Fig. 7 Raman scattering spectra of Rh B on (a) Ag thin film and as-ablated samples with laser power from 2 W to 10 W, (b) the errors bars of Raman intensity of Ag thin film and the as-ablated samples, (c) Ag thin film and as-ablated samples after 90 days from fabrication, (d) the errors bars of Raman intensity of Ag thin film and as-ablated samples after 90 days from fabrication, (e) the Raman band intensity at 1361, 1504 and 1648 cm^{-1} of Ag thin film and as-ablated sample at

different days. (f) Raman scattering spectra of Rh B on Ag thin film and as-ablated samples with various laser powers.

During the laser ablation, the surface of Ag NPs were gradually oxidized due to the elevated temperature generated by the laser energy. Ag-Ag_2O composite structure would prevent the SERS substrate from being further sulfurated and oxidized, and enhanced the stability of the SERS substrate. Nevertheless, both the nonuniform stacking of NPs and excessive oxidation will degrade the SERS performance of as-ablated samples as shown in Fig. 7(f). The Raman signal intensity of as-ablated samples increased with the laser power up to 10 W and then abruptly decreased with further increase of laser power. Therefore, it is estimated that the threshold of laser power to fabricate excellent SERS substrate is 10 W in this study.

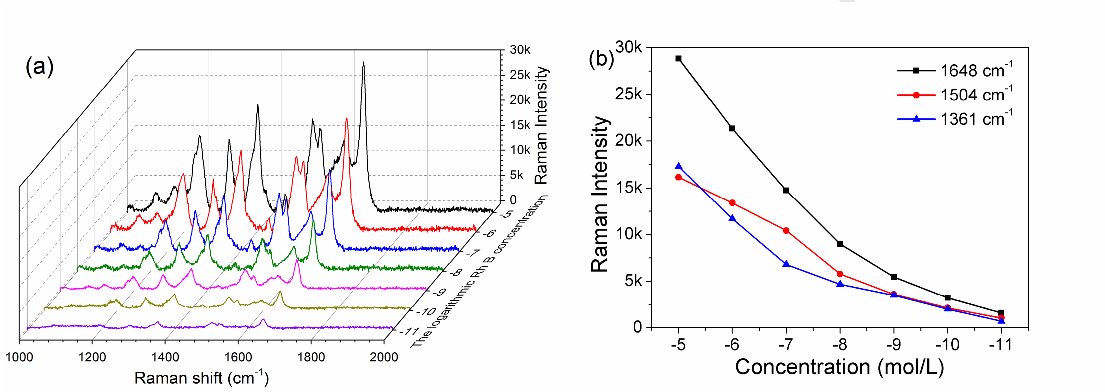

Fig. 8 (a) SERS spectra for Rh B of different concentrations ranging from 10^{-5} to 10^{-11} mol/L on as-ablated sample, (b) dependence of intensities of the 1648, 1504 and 1361 cm^{-1} Raman peaks on concentrations.

Fig. 8(a) shows the SERS performance of as-ablated sample with laser power of 10 W at different concentrations ranging from 10^{-5} to 10^{-11} mol/L. According to Fig. 8(b), the intensity of the three strongest Raman peaks of as-ablated sample decreases with the Rh B concentration decreasing. The lowest concentration of Rh B solution that can be detected is 10^{-11} mol/L, which is far below the detection limit of normal Raman spectroscopy (~0.01 mol/L) [30].

The SERS effect is due to the fact that the Raman signal of the analyte is amplified by several orders of magnitude when the analyte is at or very close to the metal nanostructure [31]. It is generally accepted that the enhancement of electromagnetic field plays a significant role in SERS effect, and that it mainly relies on the effect caused by LSPR [32]. Combined with the absorption curve, all the as-ablated samples exhibited obvious LSPR phenomena, resulting in a stronger Raman signal intensity. Recently, Mohammad Y. Khaywah et al. reported the relationship between the LSPR frequency and the SERS sensitivity [6]. They reported the intensity of Raman signal is inversely proportional to $\Delta\lambda$, which indicates the absolute value of the difference between the plasmon resonance peak position and the excitation wavelength (633 nm) of Raman spectroscopy. As the laser power increases, the absorption peak shifts to a longer wavelength where is close to the Raman excitation wavelength, which contributes to the increase of Raman intensity. Besides, the plasmon-enhanced Raman spectroscopy is strongly dependent on the aggregation of NPs [33]. According to Fig. 5(a)-(e), with the spacing of NPs decreasing, the state of aggregation increasing, the electromagnetic coupling between particles was greatly enhanced, which leaded to the enhancement of SERS signal [34].

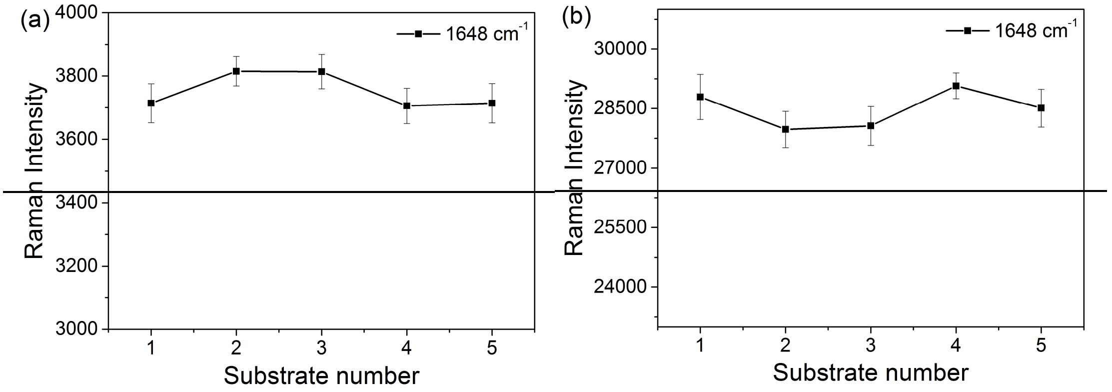

Fig. 9 The errors bars of intensity for 1648 cm^{-1} Raman peak on (a) five different Ag thin films and (b) five different as-ablated samples with laser power of 10 W.

The Raman signal intensity of 1648 cm^{-1} peak was chosen as the reference to research the reproducibility and the uniformity of samples. Five as-deposited Ag thin films and five as-ablated samples modified under laser power of 10 W were measured by the same method, as shown in Fig. 9. The intensity of 1648 cm^{-1} Raman peak for twelve different points were recorded at random on each sample. The relative standard deviation of the measured values of all samples was less than 2%, indicating that the point-to-point Raman strength of the sample was basically consistent. At the same time, the average Raman signal strength of the samples from different batches was almost the same. This means that both the as-deposited Ag thin film and the as-ablated samples have good uniformity and repeatability.

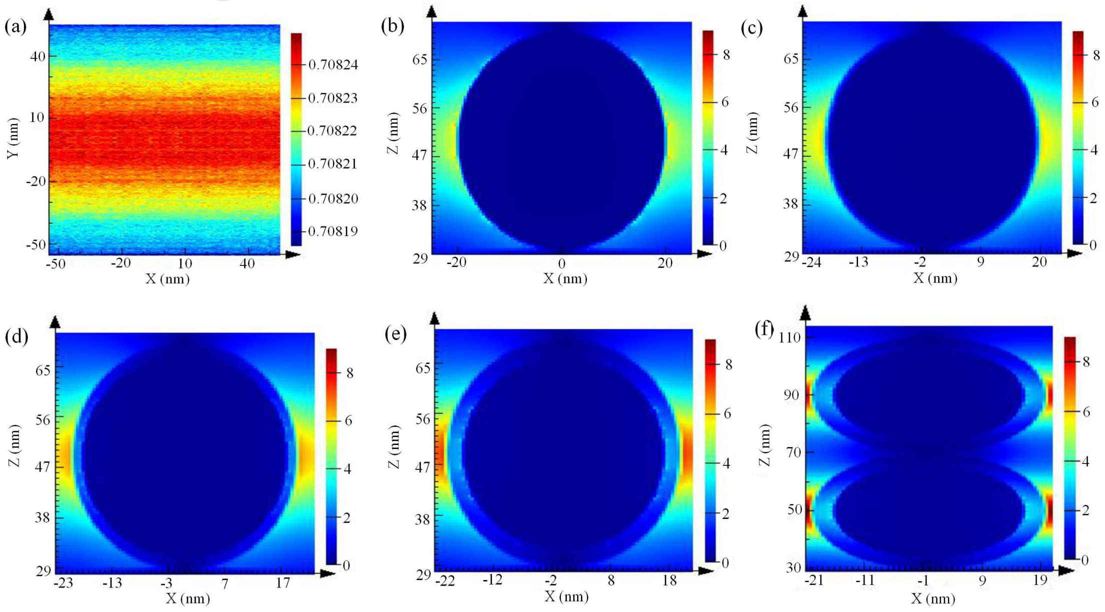

Fig. 10 FDTD simulated electric field amplitude patterns for (a) Ag thin film and (b)-(f) as-ablated samples.

Fig. 10(a)-(i) illustrate the electric field intensity in Ag thin film and as-ablated samples. In this simulation, the polarized 633 nm laser along the y-axis irradiates vertically to the x-y plane of the samples. According to Fig. 10(a), the intensity electric field of Ag film with 100 nm thickness is weaker compared with those of the structure with NPs (Fig. 10(b)-(f)). According to Fig. 10(b)-(f), the diameters of the Ag-Ag_2O composite NPs were set as 40 nm, the diameters of the Ag core were set as 40, 38, 34, 34, 32 nm, and the spacings between NPs were set as 5, 4, 3, 2, 1 nm, and the thicknesses of the Ag_2O shell were set as 0, 1, 2, 3, 4 nm, respectively. The electric field distributions of composite NPs are shown in Fig. 10(b)-(e), simulating the effects of different laser powers on both the surface oxidation degree and spacing of NPs, which can be realized by two types of parameter setting: decreasing the spacing of NPs and the thickness of Ag_2O on the surface, simultaneously. In order to match the surface morphology of the stacked particles in Fig. 5(e), the double-nanoparticle stack structure was simulated in Fig. 10(f). According to Fig. 5(f), when the laser power is over 10 W, the as-ablated sample no longer exhibits a uniform surface morphology, and a large number of particles are clustered together, so FDTD cannot be suitable for simulation. The tips or “hot spots”, aggregation of the red spots on local surface in the pictures, indicates the Raman signal for NPs structure. Evidently, the electric field intensity increases with the decrease of spacing or the increase of Ag_2O thickness. And the double-nanoparticle stacked structure has the strongest electric field intensity. The FDTD calculation results indicate that the smaller NPs spacing results in the enhancement of the Raman signal intensity. Meanwhile, the evenly distributed double-nanoparticle stack structure had preferable SERS performance than the single NPs.

4. Conclusions

In conclusion, laser-induced ablation, a cost-effective and convenient technique, was employed to fabricate Ag-Ag_2O composite structure as ultrastable SERS substrate. The Ag-Ag_2O composite structure exhibits excellent sensitivity with a detection limit of 10^{-11} mol/L for Rh B molecule solution. The oxidation degree and the spacing dependent LSPR frequency and resonance absorption intensity of Ag NPs weretuned by varying laser power. The SERS performance of samples is consistent with those results of FDTD simulation. This study provides a scalable and facile route to fabricate Ag-Ag_2O composite structure and to tune its LSPR properties, which might play a crucial part in the development of plasmonic and other applications.

Acknowledgments

This work was partially supported by the National Natural Science Foundation of China (61775140, 61775141), and the Shanghai Foundation for Science and Technology Innovation Action Plan (15441902302, 1714220060).

References

[1] P.K. Kuiri, J. Alloys Compd. 826 (2020) 154250.
[2] E. Ozbay, Science 311 (2006) 189-193.
[3] Y. Oh, M. Lee, Appl. Surf. Sci. 399 (2017) 555-564.
[4] R. Moradian, M. Saliminasab, Plasmonics 13 (2018) 1143-1151.
[5] L.A. Austin, M.A. Mackey, E.C. Dreaden, M.A. El-Sayed, Arch. Toxicol. 88 (2014) 1391-1417.
[6] M.Y. Khaywah, S. Jradi, G. Louarn, Y. Lacroute, J. Toufaily, T. Hamieh, P. Adam, J. Phys. Chem. C 119 (2015) 26091-26100.
[7] L. Yang, X. Jiang, W. Ruan, J. Yang, B. Zhao, W. Xu, J. R.Lombardi, J. Phys. Chem. C 113 (2009) 16226-16231.
[8] C. Cheng, B. Yan, S.M. Wong, X. Li, W. Zhou, T. Yu, Z. Shen, H. Yu, H.J. Fan, ACS Appl. Mater. Interfaces 2 (2010) 1824-1828.
[9] E. Fazio, F. Neri, S. Savasta, S. Spadaro, S. Trusso, Phys. Rev. B 85 (2012) 195423-195427.
[10] P. Mulvaney, Langmuir 12 (1996) 788-800.
[11] Y. Xia, N. J.Halas, MRS Bull. 30 (2005) 338-348.
[12] Y. Yao, P.T. Hoang, T. Liu, J. Mater. Sci. Technol. 33 (2017) 869-873.
[13] Hong R, Sun W, Liu Q, Li Z, Tao C, Zhang D, Zhang D (2019) Al-induced tunable surface plasmon resonance of Ag film by laser irradiation. Appl Phys Express 12:085503.
[14] P. Zimmermann, A. Hötger, N. Fernandez, A. Nolinder, K. Müller, J.J. Finley, A.W. Holleitner, Nano. Lett. 19 (2019) 1172-1178.
[15] W. Guo, B. Liu, ACS Appl. Mater. Interfaces 4 (2012) 7036-7042.
[16] O. Olea-Mejíaa, M. Fernández-Mondragóna, G.R. Conchaa, Appl. Surf. Sci. 348 (2015) 66-70.
[17] W. Soliman, N. Takada, K. Sasaki, Appl. Phys. Express 3 (2010) 03521.
[18] Petrov, P.B. Barna, L. Hultman, J.E. Greene, J. Vac. Sci. Technol. A 21 (2003) S117-S128.
[19] T. Kaspar, T. Droubay, S. Chambers, P. Bagus, J. Phys. Chem. C 114 (2010) 21562-21571.
[20] Ferraria A, Carapeto A, Rego A (2012) X-ray photoelectron spectroscopy: Silver salts revisited. Vacuum 86:1988-1991.
[21] F. Mafune, J. Kohno, A.Y. Takeda, T. Kondow, H. Sawabe, J. Phys. Chem. B 104 (2000) 9111-9117.
[22] S.J. Henley, J.D. Carey, S.R.P Silva, Phys. Rev. B 72 (2005) 195408.
[23] A.O. Altun, S.K. Youn, N. Yazdani, T. Bond, H.G. Park, Adv. Mater. 25 (2013) 4377.
[24] L. Yan, Y. Yan, L. Xu, R. Ma, F. Jiang, X. Xu, Appl. Surf. Sci. 367 (2016) 563-568.
[25] S.K. Mandal, R.K. Roy, A.K. Pal, J. Phys. D: Appl Phys 36 (2003) 261.
[26] P.B. Johnson, R.W. Chrusty, Phys. Rev. B 6 (1972) 4370-4379.
[27] T.R. Jensen, M.D. Malinsky, C.L. Haynes, R.P.V. Duyne, J. Phys. Chem. B 104 (2000) 10549-10556.
[28] P.K. Jain, M.A. El-Sayed, Chem. Phys. Lett. 487 (2010) 153-164.
[29] Y. Yang, J. Shi, G. Kawamura, M. Nogami, Scr. Mater. 58 (2008) 862-865.
[30] W. Yue, Y. Yang, Z. Wang, J. Han, A. Syed, L. Chen, K. Wong, X. Wang, J. Phys. D: Appl. Phys. 45 (2012) 425401.
[31] S. Y. Ding, J. Yi, J.F. Li, B. Ren, D.Y. Wu, R. Panneerselvam, Z.Q. Tian, Nat. Rev. Mater. 1

(2016) 16021.

[32] M. Kahraman, A. Ozbay, H. Yuksel, R. Solmaz, B. Demir, H. Caglayan, Plasmonics 13 (2018) 785-795.

[33] R.F. Aroca, Phys. Chem. Chem. Phys. 15 (2013) 5355-5363.

[34] J.M. McMahon, S. Li, L.K. Ausman, G. C. Schatz, J. Phys. Chem. C 116 (2012) 1627-1637.

Highlights:

1. Tunable LSPR property of Ag-Ag_2O composite structure was realized by using Nd:YAG fiber pulsed laser ablation.

2. SERS intensity was enchanced due to the LSPR performance of Ag-Ag_2O composite structure by increasing laser power.

3. Ag-Ag_2O composite structure has good stability and sensitivity as SERS substrates.

4. The simulation results of FDTD regarding the electric field distribution of samples are consistent with those of experiments.

Declaration of interest statement

We declare that we have no financial and personal relationships with other people or organizations that can inappropriately influence our work; there is no professional or other personal interest of any nature or kind in any product, service and/or company that could be construed as influencing the position presented in, or the review of, the manuscript entitled.